Parameter Estimation in a Model of the Human Circadian Pacemaker Using a Particle Filter

Jochem Bonarius , Charikleia Papatsimpa , and Jean-Paul Linnartz

***Abstract**—**Objective:** In the near future, real-time estimation of peoples unique, precise circadian clock state has the potential to improve the efficacy of medical treatments and improve human performance on a broad scale. Human-centric lighting can bring circadian-rhythm support using biodynamic lighting solutions that sync light with the time of day. We investigate a method to improve the tracking of individual's circadian processes. **Methods:** In literature, the human circadian physiology has been mathematically modeled using ordinary differential equations, the state of which can be tracked via the signal processing concept of a Particle Filter. We show that substantial improvements can be made if the estimator not only tracks state variables, such as the phase and amplitude of the circadian pacemaker, but also fits specific model parameters to the individual. In particular, we optimize model parameter τ_x, which reflects the intrinsic period of the circadian pacemaker (τ). We show that both state and model parameters can be estimated based on minimally-invasive light exposure measurements and sleep-wake state observations. We also quantify the effect of inaccuracies in sensing. **Results:** We demonstrate improved performance by estimating τ_x for every individual, both with artificially created and human subject data. Prediction accuracy improves with every newly available observation. The estimated τ_x-s correlate well with the subjects' chronotypes, in a similar way as τ correlates. **Conclusion:** Our results show that individualizing the estimation of model parameters can improve circadian state estimation accuracy. **Significance:** These findings underscore the potential improvements in personalized models over one-size fits all approaches.*

***Index Terms**—Circadian rhythm, particle filter, parameter estimation.*

I. Introduction

THE timing in several physiological processes in humans, including the sleep/wake cycle, hormone secretion, and

Jochem Bonarius is with the Department of Electrical Engineering, Eindhoven University of Technology.

Charikleia Papatsimpa is with the Department of Electrical Engineering, Eindhoven University of Technology, Eindhoven 5612 AP, The Netherlands (e-mail: c.papatsimpa@tue.nl).

Jean-Paul Linnartz is with the Department of Electrical Engineering, Eindhoven University of Technology, and also with Signify.

subjective alertness and performance is controlled by a biological clock, called the circadian pacemaker [1]. On its own, this pacemaker oscillates with a near-24 h period, hence the name coming from the latin words "circa" and "diem" meaning "approximately" and "a day". But the pacemaker will also synchronize to several external 'zeitgebers' including food intake, social interaction, and most importantly: retinal light exposure. Because of this, for millennia we have been using the daily pattern of light and dark to set the timing of the pacemaker in synchrony with the 24-hour light and dark cycle of the sun [2]. However, this natural light and dark pattern is disrupted by modern lifestyle. From data collected between 1992 and 1994, it was already determined that people on average spend 86.9% of their time indoors, where light levels are commonly much lower compared to outdoor light [3]. The excessive exposure to artificial light (electric light and light emitting screens such as smartphones or TVs) during the late evening and night, delays our circadian system and can acutely suppress melatonin levels and subjective sleepiness [4]. Furthermore, social demands, such as work hours or school times, often oblige us to set an alarm out of phase with our circadian propensity rhythm, resulting in insufficient sleep [5]. Circadian rhythm sleeping disorders such as insomnia, inefficient sleep and mismatch between sleep and circadian rhythmicity are associated with adverse mental and physical outcomes. In fact, circadian disruption has been associated with mood disorders, including depression, and with health risks such as diabetes, obesity, cardiovascular disease, and cancer [6]–[10].

Despite a growing scientific understanding of the impact of light on our wellbeing, performance, circadian rhythms and sleep, these insights cannot (yet) easily be harvested as benefits in lighting control systems. A wide-scale adaptation of Human-Centric Lighting is only possible if these insights can be captured by automatic control algorithms based on quantified and scientifically proven models on how humans perceive and experience lighting. An example of a potential future use for optimized light recipes is in [11]. Towards this direction, an essential aspect of any lighting control system based on circadian physiology is the precise monitoring of an individuals actual circadian state.

One of the major limitations of existing circadian models is that they are not tailored to individual physiological characteristics. Existing models are based on general population data, such that they represent the *average* responses of physiological processes and use the same parameter values for all individuals. Yet, evidence is accumulating for the existence of inter-individual

differences in circadian and sleep/wake-related variables, which is important to consider as we want to use the models to predict individual responses to input. The magnitude of such individual differences is often considerable and comparable to the effect sizes of many experimental and clinical interventions [12]. In this work, we propose an approach to individualize the estimation of specific parameters in a limit cycle oscillator model of the human circadian pacemaker and a model of the homeostatic sleep drive, exclusively using minimally-invasive measurements. We specifically focus on one such a model parameter, namely, the period of the circadian oscillator model τ_x. Our analysis showed that modelling the circadian pacemakers of individuals with different τ_x results in inter-individual variability in circadian phase, resulting in a different response to the same light exposure. Therefore, we make a plea to include such individual characterization into the system design and substantiate this in later sections. Attributing inter-individual differences in model parameters substantially improves the feasibility to track individual circadian state in an unobtrusive manner. This can make personalized light treatments more effective.

Because the physiological processes that control the sleep-wake rhythm are biological, they are stochastic in nature. Furthermore, the sensors used to observe an individual are not perfect. To account for these imperfections and variability in our chosen mathematical model, we treat the model state estimation as a full stochastic estimation and characterization problem. In particular, we adopt a particle filter estimator as an appropriate statistical framework. This is the preferred framework for our system: A regular Kalman filter is not suitable to handle the non-linearities of the models. Further, the extended or unscented Kalman filters are less suitable due to sparse observations. In fact, we elaborate a particle filter to estimate and track the circadian phase that has been suggested in [17]. In a particle filter, the posterior distributions are approximated using a point mass, which is realized as a weighted mixture of a finite number of 'particles,' each having discrete values. We further extend this framework to also estimate model parameters that reflect physiological differences between individuals, based on observations from the individuals responses to inputs. This allows a personalized prediction of the individual's response to light exposure. An important requirement for lighting control to be usable in practical settings, such as an office or home environment, is that it must be minimally invasive. However, current techniques for estimating the circadian state in a statistical framework based on user observations are often considerably invasive: typical physiological markers include the minimum of core body temperature, which requires the use of a rectal probe or telemetric pill, and/or melatonin secretion, which for instance requires the collection of saliva samples. The level of invasiveness of these methods prevent them from being used freely. A less invasive approach to estimate the circadian state would be to correlate it with the sleep-wake activity, which can for instance be determined using (remote) actigraphy [18]. In this work, we combine a model of the circadian pacemaker with a model of the sleep-wake switch as suggested in [19], providing a means to use these practically measurable observations. A preliminary version of this work was presented at 2018 Symposium on Information Theory and Signal Processing in the Benelux (IEEE Benelux/WIC) [20]. The initial description of the statistical framework is extended with an elaborate theoretical analysis of the proposed approach which gives objective insights of its capabilities, such as convergence time and the effect of particle count. Most importantly, we deal with the inherent sensor limitations present in any real-application. In this context, we exploit domain knowledge from field studies to develop a light error model that mimics real-life measurement error. We thoroughly investigate the impact of light measurement error on the system state. To our knowledge, this is one of the first attempts to address how sensor errors and limitations affect the system estimation performance in a real-life setting.

The main contribution of this paper are:
- A new statistical framework to estimate *both* circadian state and model parameters.
- Personalization of model parameters exclusively trained based on observations from the individuals responses to inputs, which can for instance be used for more accurate predictions of the effect of future light exposure.
- Provide a building block for one of the first attempts to non-invasive practical lighting system that assesses the possible health impact of light.
- Include a light error noise model that mimics the mismatch between retinal light exposure and light detected by light sensors. We investigate the impact of this error.

II. METHODS

A. The Two-Process Model of Sleep Regulation

As stated in the introduction, we are looking for a means to observe the circadian state of an individual through minimally invasive observations. We consider observations of the sleep-wake activity of the individual attractive, as these can be measured using external sensors. We realize a simulation framework to support this by combining a (mathematical) model of the circadian oscillator with a model of the sleep-wake propensity. This combination has been suggested and applied in the past [19], [21] and such a two-process model of sleep regulation has been popular in sleep research for several decades [22]. In the following subsections, we will review the two models, one describing the entrainment of the circadian system by light and one describing the switching between sleep and wake as a result of a drive consisting of homeostatic and circadian components.

1) Circadian Model: A number of mathematical models have been developed in order to understand and predict the behavior of the human circadian timekeeping system. We chose to represent the dynamics of the circadian rhythm using the Jewett-Forger-Kronauer (JFK) model [23]. The JFK model is widely accepted in the circadian science as it can accurately predict the effects of intensity, timing and duration of light stimuli on the human circadian pacemaker. It consists of two components: 1) a self-sustaining oscillator representing the endogenous rhythm of the circadian pacemaker and 2) a light input term B representing the effect of retinal light exposure (i.e., "photic drive") on the circadian oscillation. Unless stated otherwise, we use the default numerical values of parameters
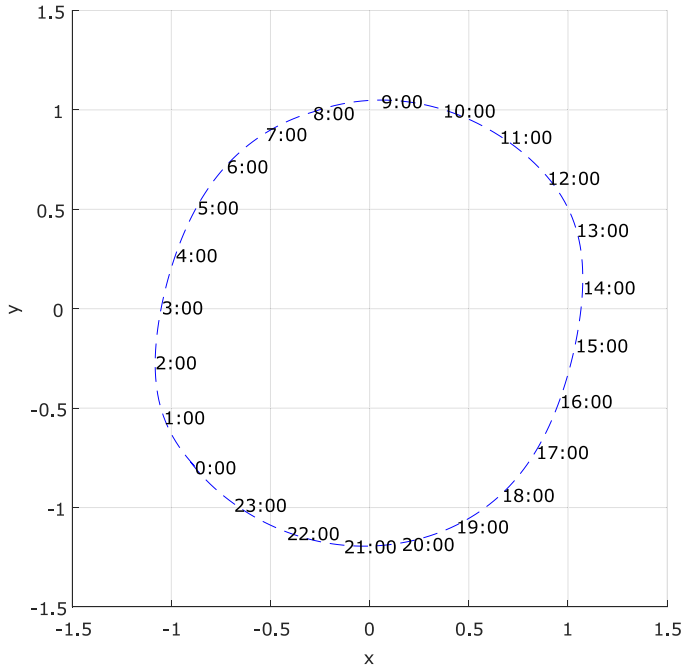
Fig. 1. Example trajectory of the two state variables x, y of the circadian pacemaker model over a 24-hour period during typical steady state conditions with the realistic light intensity profile (described near (35)).

from the original source [23]. The oscillator component of the pacemaker is modeled as a modified van der Pol oscillator which can be described by a pair of interacting state variables (x and y) described by the continuous ordinary differential equations (ODEs)

$$\dot{x} = \frac{\pi}{12}\left[y + \mu\left(\frac{1}{3}x + \frac{4}{3}x^3 - \frac{256}{105}x^7\right) + B\right] \text{ and} \quad (1)$$

$$\dot{y} = \frac{\pi}{12}\left\{qBy - \left[\left(\frac{24}{0.99729\tau_x}\right)^2 + kB\right]x\right\}. \quad (2)$$

The period of the circadian oscillator model is defined as τ_x (variable, but 24.2 h on average) and the stiffness (dampening factor) of the oscillator as μ ($\mu = 0.13$). Parameters $q = 1/3$ and $k = 0.55$ are constants.

The internal state x is the component of the circadian pacemaker that can be related to a physical indicator of the circadian state (called a biomarker), such as the endogenous core–body temperature cycle and dim-light melatonin onset, whereas y is an associated complementary variable. Together, the state variables x and y form a Cartesian coordinate pair that follows the limit cycle path of the underlying Van der Pol oscillator. An example trajectory is shown in Fig. 1.

Retinal light exposure enters the model as illuminance I (in lux) through a dynamic filtering process that represents the physiological process by which light activates the retinal photoreceptors. This process can be thought of as comprising photoreceptor activator elements that can be either in the 'ready' state (fraction $1 - n$) or the 'used' state (fraction n). Light

activates the 'ready' elements, converting them to the 'used' state at a rate α that depends on I. The most up-to-date model of the forward rate α is a multiplicative logarithmic function introduced by St. Hilaire *et al.* in [24], being

$$\alpha = \alpha_0\left(\frac{I}{I_0}\right)^p \frac{I}{I + I_1}, \quad (3)$$

where $\alpha_0 = 0.1$, $I_0 = 9500$ lx, $p = 0.5$, and $I_1 = 100$ lx. Compared to the previous model that already accurately predicts the effects of light for intensities between 150 and 9500 lux, this revision adds increased sensitivity around 100 lux, in concordance with experimental results [25].

As the photoreceptors are activated, they generate a drive onto the pacemaker, $\hat{B}$, which is proportional to the element flux rate $\alpha(1 - n)$.

$$\hat{B} = G\alpha(1 - n), \quad (4)$$

where $G = 37$ is the scaling constant and n the fraction of elements in the system that are used. Used elements are recycled back into the ready state at a rate of $\beta = 0.007$ and the rate at which elements are activated (processed from 'ready' to 'used') is given by the ODE

$$\dot{n} = 60(\alpha(1 - n) - \beta n). \quad (5)$$

Finally, the strength of the direct photic drive B is dependent on the state variables x and y such that

$$B = \hat{B}(1 - bx)(1 - by) \quad (6)$$

with $b = 0.4$, which characterizes the feature that the human circadian pacemaker has varying sensitivity to light throughout the circadian day.

To express the state x and y into a single circadian clock state C, it is projected onto a single dimension. C is used as an input for the model of the sleep homeostat explained in the next subsection. To generalize previous work, we use

$$C = 0.5(1 + c_x x - c_y y). \quad (7)$$

As stated before, the combination of the circadian- and the homeostatic model was already investigated in [19], where they used $c_x = 1$ and $c_y = 0$. Later, Skeldon *et al.* found that a phase shift was required to reproduce typical observed values for sleep duration and timing under realistic light conditions, for which they determined $c_x = 0.8$ and $c_y = -0.47$ [21, suppl. mat.]. While the previous authors both use the simplified Kronauer model [26], we are using the full JFK in an attempt to get a more accurate result, which required us to re-evaluate the values in the equation. We determined our specific values of this equation experimentally, by observing the estimated τ_x when feeding the model with light data from the field study. Although the relationship was not fully linear, we found a good compromise with a phase shift of -2.75 hours, which through conversion with Euler's formula lead to $c_x = 0.75$ and $c_y = -0.66$.

2) Homeostatic Model: The second model in our system describes the physiological need for sleep, known as homeostatic sleep pressure. This sleep pressure builds up during wakefulness and dissipates during the time the person is sleeping. For our

system, we adopt the Phillips-Robinson model [27]. In our description of the model, all parameter values except ν_{vc} and μ_H are taken from [19]. In [21] it was stated that ν_{vc} and μ_H are age dependent. The values show in this text slightly deviate from the values suggested by Skeldon *et al.*, but we found they best match the data in our field study (Section III-B). The model starts by describing how sleep- and wake states occur as a result of mutual interaction between sleep-promoting and wake-promoting neurons as described by the ODEs for their mean electric potential, V_v and V_m, respectively

$$\dot{V}_v = \frac{1}{\tau_v} \left(D_v - V_v - \nu_{vm} Q_m \right) \text{ and} \tag{8}$$

$$\dot{V}_m = \frac{1}{\tau_m} \left(D_m - V_m - \nu_{mv} Q_v \right), \tag{9}$$

where parameters $\tau_v = \tau_m = 1/360$ h are time constants of the neuronal process and the parameters $\nu_{vm} = 2.1$ m V s, $\nu_{mv} = 1.8$ m V s weight the input from population m to v and v to m respectively. Wake-promoting drive $D_m = 1.3$ m V is constant, while sleep-promoting drive D_v is determined by

$$D_v = A_v - \nu_{vc} C + \nu_{vh} H, \tag{10}$$

with $A_v = -10.2$ m V, $\nu_{vc} = 2.9$ m V, and $\nu_{vh} = 1$ m V · nM^{-1}. In (8) and (9), the neuron firing rates Q_m and Q_v are described by the logistic functions

$$Q_i = \frac{Q_{\max}}{1 + \exp\left(\frac{\theta - V_i}{\sigma}\right)}, \text{ for } i \in \{v, m\}, \tag{11}$$

which describe the relationship between the potential and the firing rate of the neurons. Here, subscript v stands for sleep-promoting- and m for wake-promoting neurons, respectively. Furthermore, $Q_{\max} = 100 s^{-1}$ is the maximum possible firing rate, $\theta = 10$ m V is the mean firing threshold, and $\sigma = 3$ m V is the standard deviation of θ. The homeostatic sleep pressure H is modeled as the virtual level of a somnogenic chemical such as adenosine and described by the ODE

$$\dot{H} = \frac{1}{\chi} \left(\mu_H Q_m - H \right), \tag{12}$$

with $\chi = 45$ h and $\mu_H = 4.0$ nM · s. Finally, wake-up and sleep-onset events are represented using the Heaviside step function $\mathcal{H}(\ldots)$

$$S = \mathcal{H}(Q_m - Q_{th}) = \begin{cases} 1 (\text{awake}), & \text{if } Q_m \geq Q_{th} \\ 0 (\text{sleeping}), & \text{otherwise} \end{cases}, \tag{13}$$

which effectively means that a person is awake when the firing rate of wake promoting neurons Q_m is equal-or-greater than a threshold value $Q_{th} = 1\tilde{\ }s^{-1}$. It is evident that a wake-up event occurs on a 0-to-1 transition of S and a sleep-onset event occurs on a 1-to-0 transition of S. Thus, the output of the combined models can be defined in the form of a set of the sleep-onset/wake-up events that occurred since the start of evaluation (i.e., at day 1, 0:00).

$$T = \{t : Q_m(t) = Q_{th}\} \tag{14}$$

For example, consider $T = \{7:50, 23:45, 32:15, 49:00, 57:00, 72:00\}$ represents a little over 3 days of evaluated time. Within
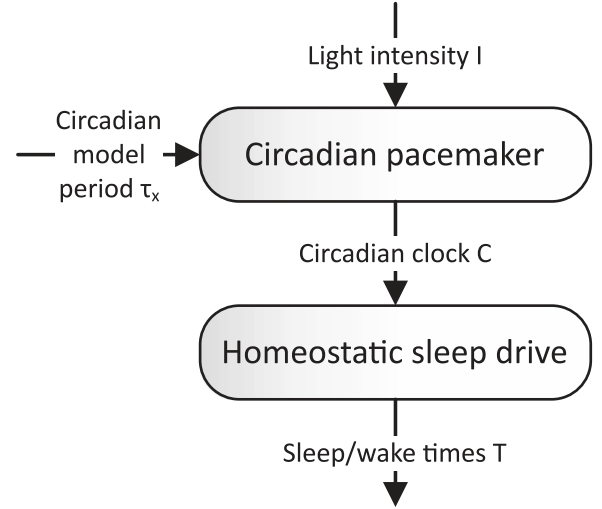

Fig. 2. Block diagram showing the model order. Light exposure enters the JFK model of the circadian pacemaker, in which the period of the circadian oscillator model τ_x is a parameter considered variable. The model produces a circadian clock that is fed to the Phillips-Robinson model of the homeostatic sleep drive. From that, the sleep-to-wake and wake-to-sleep transitions are detected, which form the output of the combined models: the time(s) at which a sleep-onset- and/or wake-up event occurs.

this set, the wake-up event times are subset $T_{\text{wake-up}} = \{7:50, 32:15, 57:00\}$ and the sleep-onset event times are subset $T_{\text{sleep-onset}} = \{23:45, 49:00, 72:00\}$. The way that the two models are connected is shown schematically in Fig. 2.

B. Particle Filter With Parameter Estimation

Both models introduced in the previous section address the effect of physiological processes that are directly or indirectly affected by external sources, in particular by light. It is commonly known that biological processes are stochastic in nature: their outcomes vary in a random manner. Furthermore, sensors that are used to measure inputs and outputs are also not perfect. However, neither the JFK, nor the Phillips-Robinson model seems to consider process uncertainties or measurement imperfections. To improve their suitability for our purpose, we introduce statistical effects into the mathematical framework. As we argued in [20], for ease of notation, we firstly combine the ODE state variables into a vector

$$\mathbf{x} = \left[n, x, y, V_v, V_m, H\right], \tag{15}$$

where our state vector $\mathbf{x}$ in bold should not be confused with the use of x which we adopted from the JFK model's original paper.

Next, we combine the circadian model with the model of the sleep homeostat, to form a single (non-linear) state-space equation

$$\dot{\mathbf{x}}(t) = F_c \left(\mathbf{x}(t), \theta(t), \mathbf{u}(t), \mathbf{v_x}(t)\right), \tag{16}$$

where $F_c(\cdots)$ is the collection of ODE equations 1, 2, 5, 8, 9, and 12 with implicit support from the other model equations. Individual specific parameters are captured in θ. In this paper,

only the period of the circadian oscillator model τ_x will be considered. However, we explicitly acknowledge that we estimate it on the fly, thus we allow a time-dependent, hopefully converging estimate $\theta(t)$. $\mathbf{u}(t)$ represents the control input vector; in our case only the [retinal] light exposure I is considered. $\mathbf{v_x}(t)$ represents the state noise (also called process noise) vector.

In practice, we cannot solve the system analytically, due to the high level of non-linearity of the equations. Instead, we integrate the equations numerically using an ODE solver. This discretizes the time steps of the state progression equations, according to

$$\dot{\mathbf{x}}_k = F\left(\mathbf{x}_{k-1}, \theta_{k-1}, \mathbf{u}_{k-1}, \mathbf{v}_{\mathbf{x},k-1}\right). \tag{17}$$

In our system, we assume that state noise, also known as process noise is caused by the stochastic nature of the biological processes. It is partially caused by the natural variation of the physiological processes, but it also simulates the effects of other mechanisms that affect the circadian clock that we do not observe, such as food intake [28] and social interaction [29]. Moreover, modeling of noise facilitates a particle filter algorithm in its operation, e.g. [17]. For our purpose, a Normal (Gaussian) distribution will adequately approximate the state noise, giving

$$\mathbf{v}_{x,k} \sim \mathcal{N}_6\left(0, \sigma_{\mathbf{x}}^2 \mathbf{I}_6\right), \tag{18}$$

where $\mathbf{I}_n$ represents the n-dimensional identity matrix and $\mathcal{N}_n(M, \Sigma)$ represents the notation for a multivariate (i.e., n-dimensional, with $n = 1$ when n is omitted) normal distribution with mean vector M and covariance matrix Σ. It can be argued that it may not be realistic to give the six state variables (in (15)), each with different value ranges, the same noise. This seems to be a pragmatic choice that appeared to work empirically. That is, it allows an otherwise rigid mathematical model to follow the spread and deviations in real biological processes of the human subjects. However, lacking a model of the spread in the human processes, we needed to empirically search for an appropriate value. We experimentally found that $\sigma_{\mathbf{x}} = 0.02$ gives us a good balance between convergence rate and the situation where too little particle spread causes the filter to stop converging short of the final value. To further address the above concerns, we later on introduce input measurement noise as well.

Next, we introduce the Bayesian statistical framework, in which we describe the state evolution as a probabilistic model. We determine that (17) represents a Markovian dynamic model of order one, where new state $\mathbf{x}_k$ is a random variable conditional on the previous state $\mathbf{x}_{k-1}$. We can then describe a state transition density function according to

$$P\left(\mathbf{x}_k | \mathbf{x}_{k-1}, \mathbf{u}_{k-1}, \theta_{k-1}\right)$$
$$= \mathcal{N}_6\left(\mathbf{x}_k | F\left(\mathbf{x}_{k-1}, I_{k-1}; \tau_{x,k-1}\right), \sigma_{\mathbf{x}}^2 \mathbf{I}_6\right), \tag{19}$$

where $\mathcal{N}_n(X|M, \Sigma)$ represents the multivariate (i.e., n-dimensional, $n = 1$ when n is ommitted) Gaussian probability density function, according to

$$\mathcal{N}_n\left(X|M, \Sigma\right) = (2\pi)^{-n/2} |\Sigma|^{-1/2}$$
$$\times \exp\left(-\frac{1}{2}(X - M)^{\mathrm{T}} \Sigma^{-1}(X - M)\right), \tag{20}$$

where superscript T denotes the matrix transpose operator.

In this paper, 'outputs' are observations on the human subject that allow the particle filter to verify the simulated state against an individual's actual (in vivo) state, observed through biomarkers. In our statistical framework, we denote the observation as a random variable z. This observation represents the time instant at which a sleep-onset or wake-up event occurs. We will use a state-space equation to represent how such an event is triggered by the current state $\mathbf{x}_k$, according to

$$z_k = K\left(\mathbf{x}_k, v_{z,k}\right), \tag{21}$$

where $v_{z,k}$ represents the output noise. The output function $K(\cdots)$ is derived from (14), in that z_k will represent a sleep-onset or wake-up event time. However, z_k interacts only very sparsely. For example, consider a z_i occurs when a person wakes up at 8:00 and the next z_{i+1} occurs when the person goes to sleep at 23:45. In practice, we will numerically integrate (16) until $Q_m = Q_{th}$ (from (13)), thereby producing a sleep-onset/wake-up event time z_k.

Similar to the state noise, we assume that the output noise is Gaussian, according to

$$v_{z,k} \sim \mathcal{N}\left(0, \sigma_z^2\right). \tag{22}$$

Currently, we are only considering the (self-recorded) sleep-onset and wake-up times as output. But self-recorded times are known not to be very accurate. For the experimental data used in this paper, we observe that test subjects will for instance record the time that they go to bed, instead of the actual sleep-onset time, which will likely be past that recorded time (This is expected behavior and is called sleep-onset latency). Furthermore, we found that individuals often tend to round-off the time to the half- or quarter-of-an-hour. Comparing recorded sleep-wake times with actigraphy data gives us a good indication of how to model this: we chose to fix the standard deviation of the output noise at half an hour, i.e., $\sigma_z = 0.5$ h. Relying purely on actigraphy data does not provide a solution to this problem, as the validity of this approach remains sub-optimal for some cases. If for instance, wrist actigraphy is used to record sleep, abnormal increased activity during the night might be incorrectly classified as wakefulness [18].

To next discuss the estimation process, we return to (21), and explicitly acknowledge that the observation z is a random variable conditional on the real state $\mathbf{x}$. For this, we can describe an output density function, which we approximate as being Gaussian,

$$P\left(z_k | \mathbf{x}_k\right) = \mathcal{N}\left(z_k | G(\mathbf{x}_k), \sigma_z^2\right). \tag{23}$$

As a refinement over Mott *et al.*, we consider that parameters in the model represent individual physiological differences. This is already shown in (19), where parameter distribution $P(\theta)$ is considered. Currently, we are only considering the period of the circadian oscillator model τ_x as a variable parameter, which is also reflected in (19) as dependent variable in $F(\dots)$. The target is to estimate this parameter distribution $P(\theta)$ similar to the way we estimate the state distribution $P(\mathbf{x})$. To achieve that, we use a mathematical approach from Liu and West [30]. First, we combine Bayes theorem with the Chapman-Kolmogorov

equation to separate the estimation of $P(\theta)$ and $P(\mathbf{x})$ into a sequential update steps, largely based on the description by Mott *et al.* [17]:

$$
\begin{aligned}
P\left(\mathbf{x}_k, \theta_k | z_{1:k}\right) = \int P\left(\theta_k | \theta_{k-1}, \mathbf{x}_k, z_k\right) \\
\times \frac{P\left(z_k | \mathbf{x}_k\right)}{P\left(z_k | z_{1:k-1}\right)} \int P\left(\mathbf{x}_k | \mathbf{x}_{k-1}, \theta_{k-1}\right) \\
\times P\left(\mathbf{x}_{k-1}, \theta_{k-1} | z_{1:k-1}\right) \mathrm{d}\mathbf{x}_{k-1} \, \mathrm{d}\theta_{k-1}
\end{aligned}
\tag{24}
$$

where $z_{1:k}$ means "all output observations from times 1 to k". Furthermore, in this equation:

- $P(\mathbf{x}_{k-1}, \theta_{k-1} | z_{1:k-1})$ represents the previous estimated state- and parameter distribution
- $P(\mathbf{x}_k | \mathbf{x}_{k-1}, \theta_{k-1})$ represents prediction update step of the particle filter, realized by evaluating the state transition density function (19).
- $P(z_k | \mathbf{x}_k)$ represents the measurement update step of the particle filter output density function (23).
- $P(z_k | z_{1:k-1})$ is a normalization constant [17], [31].
- $P(\theta_k | \theta_{k-1}, \mathbf{x}_k, z_k)$: as an improvement over Mott *et al.*, this term represents how the new parameter distribution depends on the (previous) parameter-, state-, and output distribution, i.e., the parameter transition density function.

The model dynamics are described by ODEs that are non-linear and that require a numerical evaluation. In fact, we cannot find a closed-form expression for the posterior distribution $P(\theta_k | \theta_{k-1}, \mathbf{x}_k, z_k)$. We adopted the mathematical approach by Liu and West [30], who propose that the posterior distribution can be approximated using a mixture of weighted kernel distributions. If we apply this to our parameter transition density function, it is described by

$$
\begin{aligned}
P\left(\theta_k | \theta_{k-1}, \mathbf{x}_k, z_k\right) \\
= \Sigma_{i=1}^{N} w_k^i \mathcal{N}_{\dim(\theta)}\left(\theta_k | m_k^i, h^2 V_k\right),
\end{aligned}
\tag{25}
$$

where $\dim(\theta)$ is the dimension of θ, which is equal to the number of parameters being estimated. In our case, only τ_x is considered, so $\dim(\theta) = 1$. For a discussion of the statistical principles behind this method, we refer the reader to the text book chapter by Liu and West [30].

In (25), the window width of the kernels is determined by h, where

$$
h^2 = 1 - \left(\frac{3\delta - 1}{2\delta}\right)^2,
\tag{26}
$$

for which a discount factor δ was suggested in the range 0.95-0.99, preferably close to 0.99 [30]. Experimentally, we found that this approach converges at a good rate particularly with $\delta = 0.91$, so $h^2 \approx 0.1$, thus slightly outside the range that [30] recommends.

Eq. (25) is designed to be realized in the particle filter. Specifically, in the equations we associate the superscript index i to the value of the i-th particle of a total of N particles. The weights of the particles represent how much a particle will contribute to the mixture. The particle weights are determined using information

from the output density (shown in (23)), with a normalization step, according to

$$
w_k^i = \frac{P\left(z_k | \mathbf{x}_k^i\right)}{\sum_{j=1}^{N} P\left(z_k | \mathbf{x}_k^j\right)}
\tag{27}
$$

Covariance matrix V_k is based on the posterior parameter mean vector $\bar{\theta}_k$ according to

$$
\bar{\theta}_k = \sum_{i=1}^{N} w_k^i \theta_{k-1}^i,
\tag{28}
$$

$$
V_k = \sum_{i=1}^{N} w_k^i (\theta_{k-1}^i - \bar{\theta}_k)(\theta_{k-1}^i - \bar{\theta}_k)^{\mathrm{T}}.
\tag{29}
$$

We can interpret m_k as a center of gravity of each kernel, which is related to the parameter vector. However, if $\mathbf{m}_k = \theta_{k-1}$, then the variance of the total mixture will be $(1 + h^2)V_k$, causing it to diverge excessively [30]. This can be corrected by shrinking $\mathbf{m}_k$ towards $\bar{\theta}_k$, according to

$$
m_k^i = a\theta_{k-1}^i + (1 - a)\bar{\theta}_k,
\tag{30}
$$

with shrinkage parameter a, given by

$$
a = \sqrt{1 - h^2}.
\tag{31}
$$

As we only consider parameter τ_x, (25) can be further reduced to a parameter update function for the individual particle. Applying the concept by Liu and West [30],

$$
\tau_{x,k}^i \sim \mathcal{N}(m_k^i, h^2 V_k).
\tag{32}
$$

C. Input Measurement Noise

The light exposure detected by the sensors does not perfectly represent the actual retinal light exposure of the individual. We acknowledge that a light sensor will have a measurement error because it is located at a different position than the eyes, e.g. [32]. Moreover, illuminance (in lux) is not the best way to measure light that influences the circadian rhythm, as suggested in e.g. [33]. As such sensor imperfections dominate the input 'noise,' independent identically distributed (i.i.d.) additive white Gaussian noise (awgn) may not dominate the measurement imperfections. Rather, we expect a systematic error. Such highly correlated error will systematically push the calculated chrono-state in a specific direction that may not coincide with reality. To model correlated errors, we searched for physical phenomena that capture such correlation. As an example, we assume orientation mismatch between the sensor and an individual's gaze will cause an certain gain and offset. Thus, we model the measured input light $\hat{I}$ to be a function of the actual light I according to

$$
\hat{I}_k^i = \max(g^i I_k + o^i, 0),
\tag{33}
$$

where g^i is the gain and o^i the offset which we draw for each specific particle i. The 'max'-operation is required to prevent negative values for $\hat{I}$. Realistic values for this gain and offset have been determined for a ceiling- or wall mounted light sensor in [32], which for a calibrated device reports a best-case non-image forming gain error of $\pm 32\%$ and an offset of $\sim 0.2\%$. To
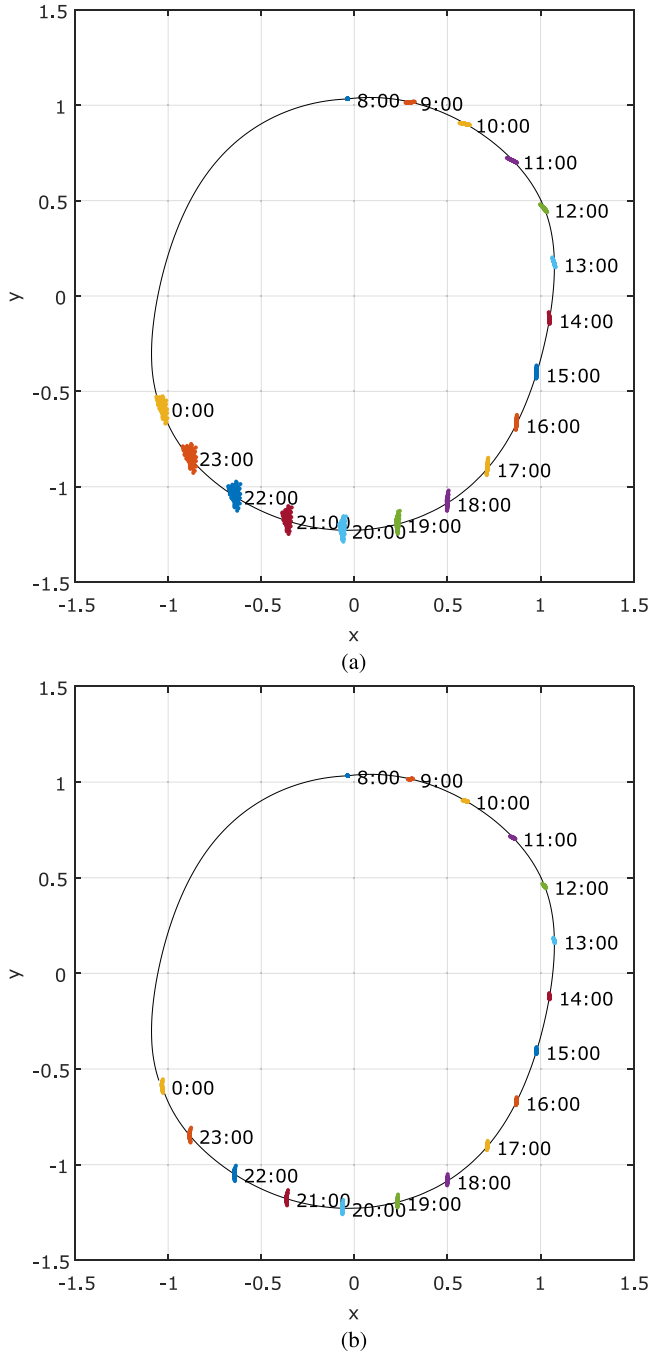
(a)

(b)

Fig. 3. The circadian state distribution spread over time due to input sensor noise, shown for an uncalibrated and a calibrated sensor. The state of the simulations are shown as points (that together form an ellipsoidal blob) for each hour from wake-up at 8:00 until sleep at 0:00, colors varying per hour. For reference, the typical state limit cycle is shown as a black solid line. (a) Uncalibrated light sensor: gain $0.5 - 2$, offset ± 20. (b) Calibrated light sensor: gain Eq. 34, offset 0.

simulate such an error we will consider this offset negligible and will draw a gain for each particle, according to

$$g^i \sim \mathcal{N}(1, (0.15)^2). \qquad (34)$$

The effect of the input noise on the state variables x and y is shown in Fig. 3 and the resulting circadian state error standard
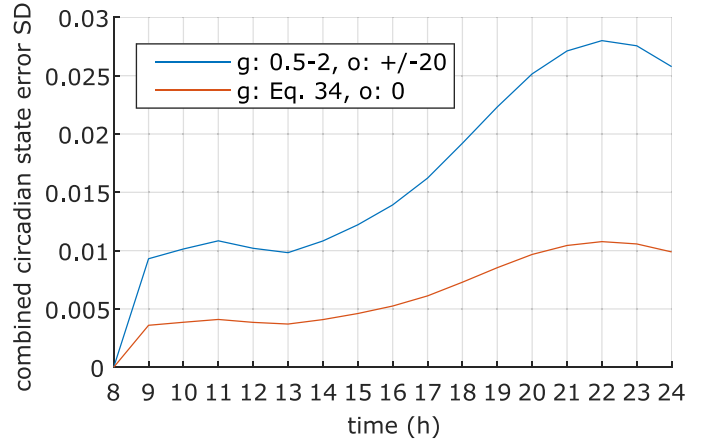

Fig. 4. Combined standard deviation of the circadian state distribution spread over time due to input sensor offset and gain errors. State noise is set to zero to isolate the effect of sensor deviations. Result of 200 simulations, each starting at wake-up at 8:00.

deviation over time is shown in Fig. 4. These results were obtained by running 200 simulations, each with different randomized gain and offset. State noise was set to zero to isolate the effect of sensor deviations. As light input, we used the realistic light profile, described near (35). The figures show that the inaccuracies of a ceiling-mounted light sensor only have a moderate impact on the circadian state, particularly when the sensor is calibrated to report the specific retinal light exposure [32].

The impact of the gain error depends on the light level, in concordance with the logarithmic light function in (3): The effect of the error will be relatively smaller for high light levels (say 10000 lx) than for low levels (say 500 lx). As we are using the realistic light profile, our light levels are in the lower range. But even when calibration leaves a substantial error ($> 30\%$), the impact on the model relatively small. This agrees with our expectation that the human entrainment to the day-night pattern is quite resilient to some light level deviations; e.g. a cloudy rather than a sunny day will not immediately de-synchronize our rhythm. We tend to conclude that light sensors with this level of imperfection are suitable as input for our system.

D. Particle Filter Initialization and Pseudo–Code

Summarizing from the previous subsections, each particle will have three properties

- the state vector $\mathbf{x}^i$.
- the parameter τ_x^i.
- the light gain (error) g^i

Starting the particle filter, these properties need to be initialized with a certain uncertainty. The light gain was already described in (34). For the τ_x we will use the suggested model mean of 24.2 and use the standard deviation 0.13 found in [13]. As the models are based around ODEs, an initialization state $\mathbf{x}_0$ is required. A state close to the actual state is preferred, although it cannot be expected the actual state is known. We determined experimentally that $\mathbf{x}_0 = [0.25, -0.9, -0.5, 2.5, -12, 13.8]$ resembles a good starting state for the data from our field study

---

Algorithm 1: Particle Filter Algorithm.

1:    **for** $i = 1 : N$ **do**
2:       Initialize:
3:       $x^i \sim$
       $\mathcal{N}_6([0.25, -0.9, -0.5, 2.5, -12, 13.8], (0.02)^2 \mathrm{I}_6)$
4:       $\tau_x^i \sim \mathcal{N}(24.2, (0.13)^2)$
5:       $g^i \sim \mathcal{N}(1, (0.15)^2)$
6:    **For each** successive output observation Z **do**
7:       **for** $i = 1 : N$ **do**
8:          **repeat**
9:            Numerically integrate $F(x^i, g^i I_k; \tau_x^i)$
10:          **until** $Q_m^i = 1$ (giving z^i)
11:      **for** $i = 1 : N$ **do**
12:        Determine particle weight
         $w^i = \mathcal{N}(z^i | Z, (0.5)^2)$
13:      Determine the total $\bar{w} = \sum_{i=1}^{N} w^i$
14:      **for** $i = 1 : N$ **do**
15:        Normalize the weight $w^i = w^i / \bar{w}$
16:      Determine parameter mean $\bar{\tau}_x = \sum_{i=1}^{N} w^i \tau_x^i$
17:      Determine parameter variance
       $V = \sum_{i=1}^{N} w^i (\tau_x^i - \bar{\tau}_x)^2$
18:      Determine new indices J using weighted sampling
       (see Algorithm 2)
19:      **for** $i = 1 : N$ **do**
20:        Draw new state, parameter, and light gain:
21:        $x'^i \sim \mathcal{N}_6(x^{J[i]}, (0.02)^2 \mathrm{I}_6)$
22:        $\tau_x'^i \sim \mathcal{N}(0.99 \tau_x^{J[i]} + 0.01 \bar{\tau}_x, 0.05\, V)$
23:        $g^i \sim \mathcal{N}(1, (0.15)^2)$
24:      **for** $i = 1 : N$ **do**
25:        Overwrite $x^i = x'^i$ and $\tau_x^i = \tau_x'^i$

Algorithm 2: Example Algorithm for Drawing New Indices With Weighted Sampling, Based on [31].

1:    Initialize CDF: $c_1 = w_k^1$
2:    **for** $i = 2 : N$ **do**
3:      Construct CDF: $c_i = c_{i-1} + w_k^i$
4:    Starts at: $i = 1$
5:    Draw a starting point: $u_1 \sim \mathcal{U}(0, N^{-1})$
6:    **for** $j = 1 : N$ **do**
7:      move along the CDF: $u_j = u_1 + N^{-1}(j-1)$
8:      **while** $u_j > c_i$ **do**
9:        $i = i + 1$
10:      Assign new index: $J[j] = i$
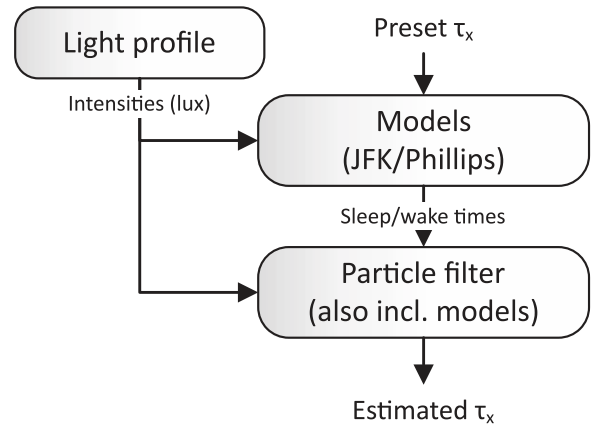11:   (Optional) shuffle J

Fig. 5. Block diagram showing the setup for the parameter estimation via simulation. The models are ran with a preset value for τ_x and with the realistic light intensity profile. This generates a set of sleep-onset- and wake-up times (See (14)). The combination of light profile and sleep-wake times are then fed into the particle filter to estimate the τ_x

(Section III-B). The state noise $(0.02)^2 \mathrm{I}_6$ was already discussed earlier.

With all the pieces of the particle filter in place, its implementation can be described by the pseudocode shown in Algorithm 1. To realize this algorithm and all simulations, we used MATLAB version 2019a (The MathWorks, Natick MA, USA). An example implementation of the method to find new indices using weighted sampling is shown in Algorithm 2, although in practice we use MATLAB's embedded function "randsample".

III. RESULTS

A. Parameter Detection in Simulation

First, we want to study the accuracy and convergence behaviour of the particle filter in estimating an individuals τ_x from only light exposure and sleep-wake rhythm. We do that by feeding the particle filter with artificially created data. For the light input we use the realistic light intensity profile as suggested by Skeldon *et al.* [21, suppl. mat.]. The intensity profile from 8:00 to 0:00 is described by

$$I(t) = l_2 + \frac{l_1 - l_2}{2} \left\{ \tanh[c(t - s_1)] - \tanh[c(t - s_2)] \right\}, \tag{35}$$

where sunrise and sunset times are $s_1 = 7.5$ resp. $s_2 = 16.5$, day and evening light intensities are $l_1 = 700$ lx resp. $l_2 = 40$ lx, and switching speed $c = 0.6\ \mathrm{h}^{-1}$. From 0:00 to 8:00 we assume darkness (0 lx).

We feed the light data to the combined JFK and Phillips models with a predetermined (to be estimated) τ_x, which generates artificial sleep-onset and wake-up times. To allow the particle filter enough time to converge, we evaluate the models equations with an ODE solver for 1 month (31 days = 744 hours) of simulated time, which produces 62 sleep-onset / wake-up event times. Next, the combination of light data and artificial sleep-onset / wake-up times is fed to the particle filter to estimate the corresponding model parameter τ_x. The system setup is shown in Fig. 5.

One key parameter of the particle filtering approach is the number of particles used to represent a distribution. This parameter defines the trade-off between computational cost and the variance of the resulting estimates at the end of the simulation time. We have to find a trade off between the rate of convergence, which is inversely proportional to the square root of the number of particles used, and the computational cost, which grows proportionally with the number of particles [34].
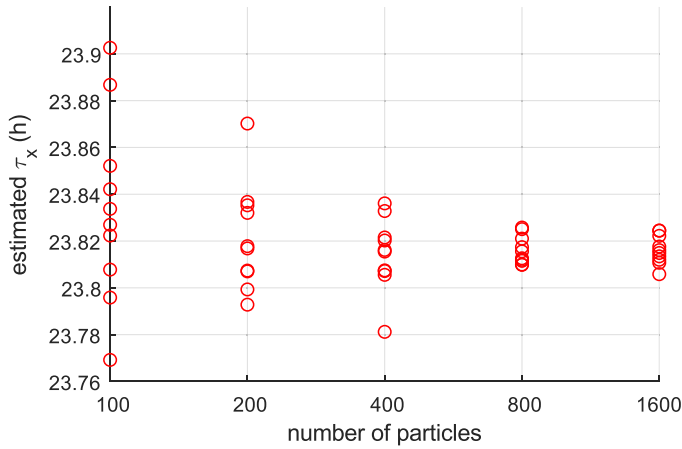
Fig. 6. The estimated τ_x-s for 10 runs each of 100, 200, 400, 800 and 1600 particles, with preset $\tau_x = 23.8$ h. For 100 to 400 particles the results are spread out significantly more than for 800 or 1600 particles. 1600 particles doesn't show improvement over 800 particles. In all cases the average detected τ_x is a bit higher than the preset value, likely caused by nonlinearities of the models.
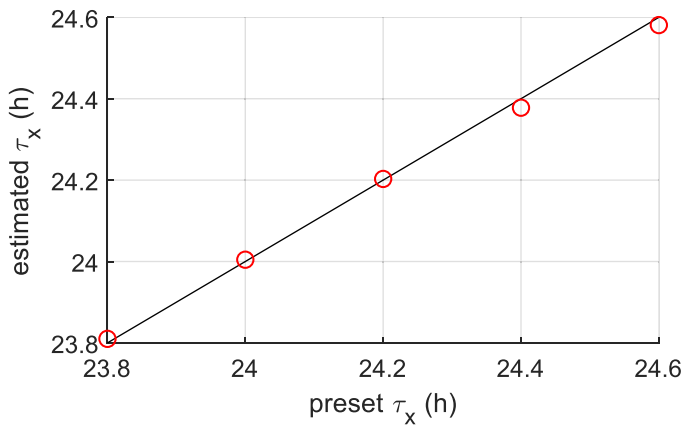

Fig. 7. The values of τ_x estimated by the particle filter with preset τ_x of 23.8, 24.0, 24.2, 24.4, and 24.6 shown as red circles. The 1-to-1 line is shown in black. Each time, the particle filter is ran with 800 particles for 31 days of artificial data.

Fig. 6 illustrates the distribution spread of the estimated τ_x at the end of the simulation as a function of the number of particles. Experimentally, we found that using 800 particles will give a good balance between computational performance and accuracy for a wide distribution of considered τ_x values. Using more particles will give approximately identical results, while requiring more processing power.

Five simulated scenarios with different preset τ_x of 23.8, 24.0, 24.2, 24.4, and 24.6 were evaluated to demonstrate the capability of the particle filter estimator to reproduce the individual circadian period.

Results presented in Fig. 7 show that the particle filter is able to detect the preset τ_x with high accuracy, although the values below 24.2 are estimated a bit higher and value above 24.2 are estimated a bit lower. Likely, this effect is caused by the nonlinearities of the models.
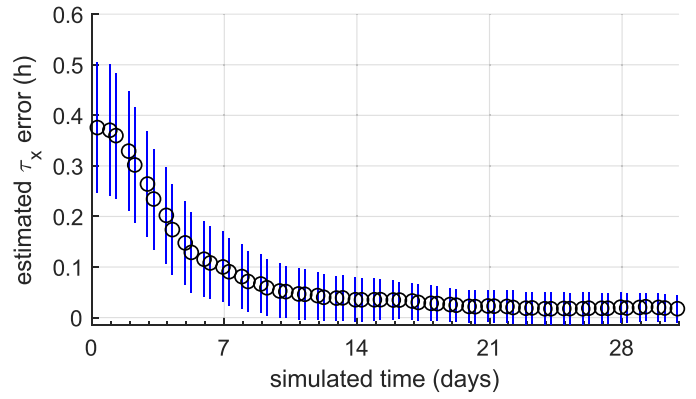

Fig. 8. Typical distribution of the estimated τ_x error with respect to the preset value over time. The preset τ_x value for this run was 23.8 and the particle filter was ran with 800 particles for 31 days. The open circles are the mean error values and the vertical lines indicate the standard deviation. These points are determined at the simulated sleep-wake times (i.e., the output observations).

An important performance indicator is the convergence of parameter estimation, in particular how the error between estimated parameters and their true value decreases during the days of observation and whether a residual error remains. A typical convergence flow of the particle filter estimator for the chosen number of particles is presented in Fig. 8. The estimation error drops with every observation update. In fact, after 7 days (168 h) the estimation error is already reduced by 75% to around 0.10 h ± 0.07 h (mean $\pm$ standard deviation) of the initial 0.4 h. Taken together, our results show that the estimated parameter τ_x converged to the true parameter value with low estimation error (Fig. 7) showing a fast convergence rate (Fig. 8). This correspondence lends confidence to the usefulness of the method in real-life scenarios where the actual parameter values will be unknown.

B. Parameter Detection With Human Data

For verification of the model against human data, data was used from an ambulatory study [35]. Twenty elderly participated in the study (12 males and 8 females, mean age = 71.18 years, SD = 3.71, age range = 65–79). Persons with moderate or more severe physical- or cognitive impairments were excluded. The latter was tested using the subscale Forgetfulness of the Cognitive Failures Questionnaire (CFQ) (mean = 75.24, SD = 8.67) [36]. Each participant wore a light logging device [37] for at least 7 days, which samples the light level every 160 seconds. The light logging device is based around the TCS34725 Color Sensor by AMS [38]. During daytime the device was clipped on the top of the shirt and during the night, the device was placed on a night stand as close to the head of the participant as possible. Additionally each participant wore a wrist-worn actigraphy device (Philips Respironics Actiwatch Pro) and maintained a sleep dairy, where they recorded their bedtimes. Both the objective measurement of the actigraphy and the subjective measurement of the sleep diary were manually combined to estimate the individuals' sleep-onset and wake-up times. Sleep was assumed in darkness and very little to no
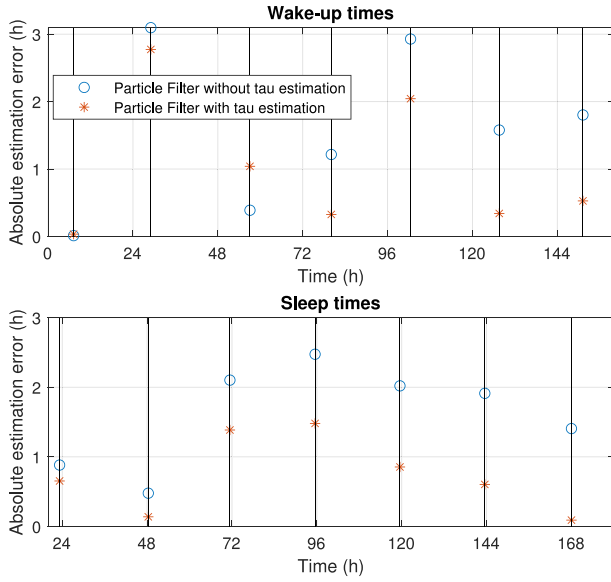
Fig. 9. Comparison of estimated wake-sleep times for of a particle filter with parameter estimation and with the use of a fixed τ_x. The estimated τ_x parameter value for this participant is 23.8 (smaller than the average 24.2.). Errors are are determined at the actual, observed sleep-wake times.

movement. We do not consider a specific sleep-onset latency. During the 7 days of recording, the participants conducted their normal day routine. None of the participants used an alarm clock. The study adhered to the declaration of Helsinki, the Code of Ethics of the NIP (Nederlands Instituut voor Psychologen - Dutch Institute for Psychologists), and national legal and ethics requirements. It was approved by the Eindhoven University of Technology's internal Ethical Review Board. Of all the collected data, 4 data sets had to be dropped due to hardware issues or user errors. We further determined each individual's chronotype according to [39, suppl. inf.]. As the participants are not using alarm clocks, their chronotype (MSFsc) is equal to the mean midsleep on free days (MSF), given by

$$\text{MSF} = \mathbb{E}[t_{\text{sleep onset}} + t_{\text{sleep duration}}/2]. \quad (36)$$

The light data and sleep-wake times were each processed by our proposed particle filter, which resulted in an estimation of daily sleep and wake-up times and parameter τ_x for each individual. To explore to what extent τ_x parameter estimation outperforms the forecasting of an individual's sleep and wake-up times, we compare the estimation performance of a particle filter with parameter estimation with one that uses a fixed τ_x. As an illustrative example, Fig. 9 shows the absolute error in the wake-up and sleep times estimation for a test participant. Our estimated τ_x deviates from the population average 24.2. Personalizing that model parameter largely improves estimation accuracy. In fact, we see that the estimation error consistently shows improved performance compared to the fixed model with preset $\tau_x = 24.2$. As our data-set is limited to 7 days, the final estimate of τ_x might not fully represent the best possible fit. Indeed, as we explicitly analyze in section III-A, in 7 days of training, the τ_x estimation error has been reduced by 75%.
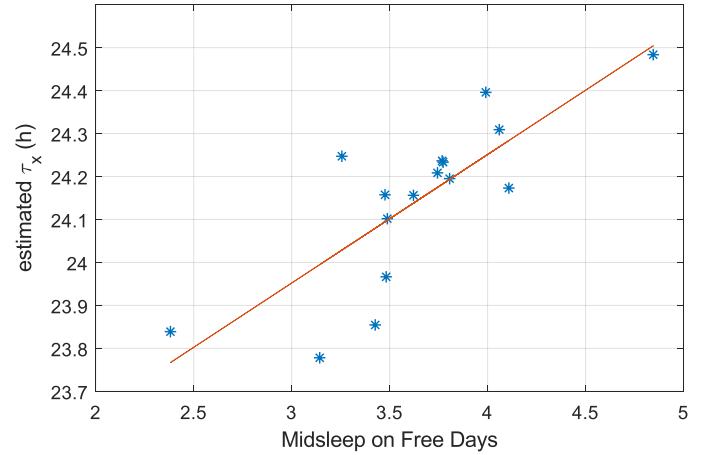

Fig. 10. The scatter plot showing the estimated τ_x versus the determined chronotype, which for our case equals to the (mean) midsleep on free days, for the data from the field study (blue stars). The linear regression line is shown in red. The Pearson coefficients are $r = 0.80$ and $p = 0.0002$.

Hida *et al.* showed that the intrinsic circadian period correlates with the MSF [40]. Interestingly, we also found a similar correlation between the individuals' τ_x found by the particle filter with the respective MSF, with the Pearson correlation coefficients having a strength of $r = 0.80$ and a significance of $p = 0.0002$, as shown in Fig. 10. This suggests that our estimate of the model parameter τ_x (period of the circadian oscillator model) is also an estimate of the physiological parameter τ, the intrinsic period of the human circadian pacemaker. However, there are challenges in individualizing model parameters to fit user-specific data. One such difficulty stems from the fact that models may display parameter dependencies, whereby estimating only a subset of parameters can compensate for the other parameters which are kept fixed, resulting in some arbitrariness in the specification of their values. In this view, our estimated τ_x may also compensate other model parameters that we did not explicitly vary. A further validation is required to verify whether our statistical approach is able to actually estimate a physiological parameter.

IV. DISCUSSION AND FUTURE WORK

In our proposed method, we simulate models of the sleep-wake regulation using data that can be observed with minimally invasive measurement methods. Specifically, we use light exposure as an input to the model, and sleep-onset and wake-up times to monitor and track the output of the model. Using this observed data, we not only extract information that indicates the actual circadian phase of the individual, but also information that indicates the value of an internal parameter of the model representing the period of the circadian oscillator model. We verify this period by correlating it against the individual's MSF, which is also derived from the sleep-onset and wake-up times. This works well for our situation.

In this work, the timing of sleep is modeled as the interaction of homeostatic and circadian components. Admittedly, a variety of internal factors, such as stress and medical conditions, and external factors, such as such as food- and caffeine intake and social

interaction, can also influence the timing of sleep. As a result, our estimated wake-up and sleep times may not necessarily match the observed sleep and wake-up times. Additionally, when an alarm clock is used, an individual will most likely not wake-up at his/her natural wake-up time. We expect that our attempt to fit model parameters to individual user observations may to some degree compensate for those other factors that influence sleep. In such case, the resulting estimated model parameters may not yield values that best represent the physiological properties of the individual. It is part of future research to find alternative biomarkers that track the circadian state, such as body temperature or heart rate variability, and integrate these into our proposed system.

The number of particles that we use in our simulation is limited. Mott *et al.* [17] suggested 240 particles was sufficient for estimating 3 variables. As we include 3 more state variables by adding the Phillips-Robinson model and also consider parameter τ_x to be variable, one could deduct that we would require somewhere in the order of $(240)^{7/3} \approx 360000$ particles. However, as shown in Section III-A we already find stable convergence with only 800 particles. Intuitively, using only 800 particles may suffice to get convergence as the initial state is close to the actual state of the circadian clock en because the state noise $\sigma_{\mathbf{x}}$ is quite small. Furthermore, the Phillips-Robinson model mostly follows the circadian state C, hence no excessive effort is required to estimate the extra state variables. Most effort seems to be going into finding the parameter τ_x, for which the relatively small number of particles is sufficient. In future research, we plan to explore the limits of the particle filter by increasing the state noise: it is expected that more particles will be required to reach convergence at a comparable rate.

During our experiments, we found a statistical deviation of the parameters that were considered age-related by Skeldon *et al.* [21]: ν_{vc} and μ_H. We expect that these parameters are not only age related, but differ between individuals of the same age. In a quick experiment (not reported here) we considered these parameters as a part of variable parameter vector θ, which improved the correlation between the estimated τ_x and the MSF. Our results suggest that these parameters should also be considered variable and are 'to be estimated' as part of θ. However, as the model has many parameters that could differ between individuals, we should carefully select which parameters are to be considered variable. Trying to estimate too many parameters with limited input data could cause the model to be over-fitted, where the resulting parameters will only be valid for the specific input data used for training. What parameters to consider in θ will be a topic for future research.

The sleep-onset and wake-up times have a different time interval: i.e., on average a persons is awake 16 hours and asleep 8 hours. Thus, one would expect the state noise σ_x to depend on k. However, as the time between *two* sleep-onset and wake-up times is 24 hours on average (i.e., $\mathbb{E}[z_{k+2} - z_k] = 24$ h) we assume the fixed-valued state noise we use is sufficiently accurate.

A key unanswered question is whether our estimate of τ_x also paves a path towards a viable, unobtrusive method to estimate an actual physiological property, namely, the intrinsic circadian period of an individual τ. Although the Forced Desynchrony protocol is regarded as the most reliable and valid method for the assessment of τ in humans, it is laborious and highly impact-full for the human subject. Having an alternative that reduces the burden on the subjects and increases the feasibility of examination, even an alternative that can be suitable for non-medical grade applications is attractive. We acknowledge that this work did not verify to what extent our method converges to the same value as a gold standard for measuring τ. For instance, another model parameter may also correlate with wake up time variations, and it is not ruled out that our τ_x-estimate takes on a optimum value that also absorbs these effects. Still, our results revealed a significant correlation between our estimates of τ_x and chronotype, in a similar way as τ correlates, but we leave it to future research to test to what extent our estimation method also is a suitable, less invasive method to estimate τ.

V. CONCLUSION

In this work, we present a novel approach to estimate both the circadian state and the model parameters of the human sleep-wake rhythm based on minimally-invasive light exposure measuments and sleep-wake state observations. Our target is to improve the accuracy of personalized predictions of the effect of future light exposure scenarios on individuals.

Initial simulation results using artificially created, but realistic, light exposures show the accuracy of the suggested method when estimating the circadian period of an individual: we determined that representing distributions using 800 particles suffice to determine τ_x with good accuracy in 31 days of simulated time. A second experiment using data collected from real human test subjects shows a significant correlation between an individuals τ_x estimated by the system and their respective MSF. As this correlation was already determined in literature, this demonstrates correct functioning of our algorithm.

Humans differ from each other. Our evaluations show that due to biological differences (e.g. spread in τ_x) different light recipes are required to achieve the same goal. That is, lighting control based on population averages will have much less effect than algorithms that take human variation into account and could even have adverse effects on certain individuals. While a further validation of our proposed algorithm against human data has not been performed, our initial results suggest that our algorithm may provide a useful tool to address inter-individual differences when determining lighting control. Therefore, our proposed method is a step towards human-centric smart lighting control systems centered around individual needs.

REFERENCES

[1] R. M. Buijs *et al.*, "The biological clock tunes the organs of the body: Timing by hormones and the autonomic nervous system," *J Endocrinol.*, vol. 177, no. 1, pp. 17–26, Apr. 2003.

[2] H. S. Lee, H. J. Billings, and M. N. Lehman, "The suprachiasmatic nucleus: A clock of multiple components," *J. Biol. Rhythms*, vol. 18, no. 6, pp. 435–449, Dec. 2003.

[3] N. E. Klepeis *et al.*, "The national human activity pattern survey (NHAPS): A resource for assessing exposure to environmental pollutants," *J. Expo. Anal. Environ. Epidemiol.*, vol. 11, pp. 231–252, 2001

[4] J. J. Gooley *et al.*, "Exposure to room light before bedtime suppresses melatonin onset and shortens melatonin duration in humans," *J. Clin. Endocrinol. Metab.*, vol. 96, no. 3, pp. E463–E472, Mar. 2011.

[5] M. Wittmann *et al.*, "Social jetlag: Misalignment of biological and social time," *Chronobiol. Int.*, vol. 23, no. 1-2, pp. 497–509, 2006.

[6] N. Antypa *et al.*, "Chronotype associations with depression and anxiety disorders in a large cohort study," *Depress. Anxiety*, vol. 33, no. 1, pp. 75–83, Jan. 2016.

[7] "Circadian Rhythms and Bipolar Disorder | Brain & Behavior Research Foundation." [Online] Available: https://www.bbrfoundation.org/event/ circadian-rhythms-and-bipolar-disorder. Accessed: Dec. 13, 2019.

[8] R. G. Stevens, "Light-at-night, circadian disruption and breast cancer: Assessment of existing evidence," *Int. J. Epidemiol.*, vol. 38, no. 4, pp. 963–970, 2009.

[9] S. Reutrakul and K. L. Knutson, "Consequences of circadian disruption on cardiometabolic health," *Sleep Med. Clin.*, vol. 10, no. 4, pp. 455–468, Dec. 2015.

[10] K. G. Baron and K. J. Reid, "Circadian misalignment and health," *Int. Rev. Psychiatry*, vol. 26, no. 2, pp. 139–154, 2014.

[11] C. Papatsimpa and J.-P. M. G. Linnartz, "Personalized office lighting for circadian health and improved sleep," *Sensors*, vol. 20, no. 16, 4569, pp. 1–17, Aug. 2020.

[12] H. P. A. Van Dongen, K. M. Vitellaro, and D. F. Dinges, "Individual differences in adult human sleep and wakefulness: Leitmotif for a research agenda," *Sleep*, vol. 28, no. 4, pp. 479–96, Apr. 2005.

[13] C. A. Czeisler *et al.*, "Stability, precision, and near-24-hour period of the human circadian pacemaker," *Science*, vol. 284, pp. 2177–2181, Jun. 1999.

[14] J. F. Duffy *et al.*, "Sex difference in the near-24-hour intrinsic period of the human circadian timing system," in *Proc. Natl. Acad. Sci.*, USA, vol. 108, suppl. 3, pp. 15602–15608, Sep. 2011.

[15] D. A. Dean, II, D. B. Forger, and E. B. Klerman, "Taking the lag out of jet lag through model-based schedule design," *PLoS Comput. Biol.*, vol. 5, no, 6, Jun. 2009, Art. no. e1000418.

[16] N. Stack *et al.*, "Estimating representative group intrinsic circadian period from illuminance-response curve data," *J. Biol. Rhythms*, vol. 35, no. 2, pp. 195–206, 2020. [Online]. Available: https://journals.sagepub.com/doi/ full/10.1177/0748730419886992

[17] C. Mott *et al.*, "Model-based human circadian phase estimation using a particle filter," *IEEE Trans. Biomed. Eng.*, vol. 58, no. 5, pp. 1325–1336, May 2011.

[18] J. L. Martin and A. D. Hakim, "Wrist actigraphy," *Chest*, vol. 139, no. 6, pp. 1514–1527, Jun. 2011

[19] A. J. K. Phillips, P. Y. Chen, and P. A. Robinson, "Probing the mechanisms of chronotype using quantitative modeling," *J. Biol. Rhythms*, vol. 25, no. 3, pp. 217–227, Jun. 2010.

[20] J. H. Bonarius and J.-P. M. G. Linnartz, "Particle filter-based parameter estimation in a model of the human circadian rhythm," in *Proc. Symp. Inf. Theory Signal Benelux*, Enschede, The Netherlands, 2018, pp. 35–45.

[21] A. C. Skeldon, A. J. K. Phillips, and D.-J. Dijk, "The effects of self-selected light-dark cycles and social constraints on human sleep and circadian timing: A modeling approach," *Sci. Rep.*, vol. 7, Mar. 2017, Art. no. 45158.

[22] A. A. Borbély *et al.*, "The two-process model of sleep regulation: A reappraisal," *J. Sleep Res.*, vol. 25, no. 2, pp. 131–143, 2016.

[23] M. E. Jewett, D. B. Forger, and R. E. Kronauer, "Revised limit cycle oscillator model of human circadian pacemaker," *J. Biol. Rhythms*, vol. 14, no. 6, pp. 493–499, Dec. 1999.

[24] M. A. St. Hilaire *et al.*, "Addition of a non-photic component to a light-based mathematical model of the human circadian pacemaker," *J. Theor. Biol.*, vol. 247, pp. 583–599, Aug. 2007.

[25] J. M. Zeitzer *et al.*, "Sensitivity of the human circadian pacemaker to nocturnal light: Melatonin phase resetting and suppression," *J. Physiol.*, vol. 526, no. 3, pp. 695–702, Aug. 2000.

[26] D. B. Forger, M. E. Jewett, and R. E. Kronauer, "A simpler model of the human circadian pacemaker," *J. Biol. Rhythms*, vol. 14, no. 6, pp. 533–537, Dec. 1999.

[27] A. J. K. Phillips and P. A. Robinson, "A quantitative model of sleep-wake dynamics based on the physiology of the brainstem ascending arousal system," *J. Biol. Rhythms*, vol. 22, no. 2, pp. 167–179, Apr. 2007.

[28] E. Challet, "The circadian regulation of food intake," *Nat. Rev. Endocrinol.*, vol. 15, pp. 393–405, May 2019.

[29] Y. Bao *et al.*, "Synchronization as a biological, psychological and social mechanism to create common time: A theoretical frame and a single case study," *PsyCh. J.*, vol. 4, no. 4, pp. 243–254, Dec. 2015.

[30] J. Liu and M. West, "Combined parameter and state estimation in simulation-based filtering," in *Sequential Monte Carlo Methods in Practice*, A. Doucet, N. de Freitas, and N. Gordon, Eds., New York, NY, USA: Springer Science+Business Media, 2001, pp. 197–223.

[31] M. S. Arulampalam *et al.*, "A tutorial on particle filters for online nonlinear/non-Gaussian Bayesian tracking," *IEEE Trans. Signal Process.*, vol. 50, no. 2, pp. 174–188, Feb. 2002.

[32] T. W. Kruisselbrink, R. Dangol, and E. J. van Loenen, "Feasibility of ceiling-based luminance distribution measurements," *Building Environ.*, vol. 172, Jan. 2020, Art. no. 106699.

[33] R. J. Lucas *et al.*, "Measuring and using light in the melanopsin age," *Trends Neurosci.*, vol. 37, no. 1, pp. 1–9, Jan. 2014.

[34] V. Elvira, J. Míguez, and P. M. Djurić, "Adapting the number of particles in sequential Monte Carlo methods through an online scheme for convergence assessment," *IEEE Trans. Signal Process.*, vol. 65, no. 7, pp. 1781–1794, Apr. 2017.

[35] R. van der Sande, "Light and elderly - The effect of light exposure on well-being and sleep in the everyday life of elderly," M.S. thesis, Dept. Social Sciences, Eindhoven Univ. Tech., Eindhoven, The Netherlands, 2017

[36] D. E. Broadbent, P. F. Cooper, P. FitzGerald, and K. R. Parkes, "The cognitive failures questionnaire (CFQ) and its correlates," *Brit. J. Clin. Psychol.*, vol. 21, no. 1, pp. 1–16, 1982.

[37] G. Martin, "Lightlog - Brighten your day," [Online] http://lightlogproject. org/ Accessed: Mar. 16, 2020.

[38] AMS, "TCS34725 Color Sensor," [Online] Available: https://ams.com/ TCS34725. Accessed: Jul. 10, 2020.

[39] T. Roenneberg *et al.*, "Social Jetlag and Obesity," *Curr. Biol.*, vol. 22, no. 10, pp. 939–943, May 2012.

[40] A. Hida *et al.*, "In vitro circadian period is associated with circadian/sleep preference," *Sci. Rep.*, vol. 3, no. 2074, pp. 1–7, Jun. 2013.